Angewandte Chemie
Eine Zeitschrift der Gesellschaft Deutscher Chemiker

Supporting Information

69451 Weinheim, Germany

Configurationally Stable Molecular Propellers: the First Resolution of Residual Enantiomers

Tiziana Benincori, Giuseppe Celentano, Tullio Pilati, Alessandro Ponti, Simona Rizzo, and Francesco Sannicolò

Experimental Section

General procedure for the preparation of phosphine oxides 1a-c: A mixture of phosphorus oxybromide (1 mmol) and pyridine (9 mmoles) was added to the suitable N-methyl-2-alkylindole (3.8 mmoles) under nitrogen. The reaction mixture was heated at 90°C under stirring for 18 h, then diluted with dichloromethane and the resulting solution exhaustively extracted with a 1N HCl solution. The organic layer was washed with H_2O, dried over Na_2SO_4 and evaporated to dryness to give a residue which was chromatographed on a silica gel column to separate the phosphine oxide **1** from unreacted N-methyl-2-alkylindole, which was eluted first.

Tris[3-(1,2-dimethylindolyl)]phosphine oxide (1a): 1,2-Dimethylindole (Aldrich [*875-79-6*]: 5.78 g; $POBr_3$: 2.85 g; pyridine (6 mL). Chromatography eluant: CH_2Cl_2/EtOH 9.5:0.5. The product was crystallized from a 1:3 mixture of $CHCl_3$/EtOAc. M.p. 270°C, 63% isolation yields; ^{1}H NMR ($CDCl_3$, 300 MHz) δ = 7.29 (broad d, J = 8.1 Hz, 1H), 7.08 (td, J_1 = 7.4 Hz and J_2 = 1.4 Hz, 1H), 6.72 (td, J_1 = 8.1 Hz and J_2 = 1.1 Hz, 1H), 6.67 (broad d, J = 7.4 Hz, 1H), 3.71 (s, N-CH_3), 2.57 (d, J = 1.34 Hz, CH_3) ; ^{31}P NMR ($CDCl_3$, 300 MHz) δ = 8.33 (s); ^{13}C NMR ($CDCl_3$, 300 MHz) δ = 145.34 (d, J = 18 Hz), 137.25 (d, J = 11.25 Hz), 128.67 (d, J = 12 Hz), 120.96 (s), 120.47 (s), 120.21 (s), 108.81 (s), 105.15 (d, J = 132 Hz), 29.58 (s), 12.24 (s); HRMS (EI) calcd for $C_{30}H_{30}N_3OP$: $[M]^+$ 479.212651, found 479.213100.

Tris[3-(2-ethyl-1-methylindolyl)]phosphine oxide (1b). 2-Ethyl-1-methylindole: 2.08 g; $POBr_3$: 1.07 g; pyridine (3 mL). Chromatography eluant: EtOAc/$CHCl_3$ 7:3. The product was crystallized from EtOAc. M.p. 244°C, 74% isolation yields; ^{1}H NMR ($CDCl_3$, 300 MHz) δ = 7.31 (broad d, J = 8.2 Hz, 1H), 7.10 (td, J_1 = 8.2 Hz and J_2 = 2.4 Hz, 1H), 6.72 (m. 2H), 3.75 (s, N-CH_3), 3.15 (q, J = 7.3 Hz, CH_2), 1.02 (t, J = 7.3 Hz, CH_3); ^{31}P NMR ($CDCl_3$, 300 MHz) δ = 7.1 (s); ^{13}C NMR

($CDCl_3$, 300 MHz) δ = 151.05 (d, *J* = 18.7 Hz), 137.75 (d, *J* = 11.7 Hz), 129.2 (d, *J* = 11.7 Hz), 121.41 (s), 121.16 (s), 120.81 (s), 109.24 (s), 105.54 (d, *J* = 130.6 Hz), 29.99 (s), 19.78 (s), 14.06 (s); HRMS (EI) calcd for $C_{33}H_{36}N_3OP$: $[M]^+$ 521.259602, found 521.258910.

Tris[3-(2-*i*-propyl-1-methylindolyl)]phosphine oxide (1c). 1-Methyl-2-*i*-propylindole: 2.76 g; $POBr_3$: 1.20 g; pyridine (3 mL). Chromatography eluant: EtOAc/$CHCl_3$ 1:1. The product was crystallized from EtOAc. M.p. 299°C, 70% isolation yields; ^{1}H NMR ($CDCl_3$, 300 MHz) δ = 7.28 (d, *J* = 8.1 Hz), 7.06 (td, J_1 = 7.6 Hz and J_2 = 1.1 Hz), 6.66 (t, *J* = 8.1 Hz), 6.52 (d, *J* = 8.1 Hz), 4.39 (heptet, *J* = 7.3 Hz, CH), 3.86 (s, N-CH_3), 1.32 (d, *J* = 7.35 Hz, CH_3), 1.07 (d, *J* = 7.35 Hz, CH_3); ^{31}P NMR ($CDCl_3$, 300 MHz) δ = 7.39 (s); ^{13}C NMR ($CDCl_3$, 300 MHz) δ = 154.00 (d, *J* = 18.1 Hz), 138.44 (d, *J* = 11.4 Hz), 129.05 (d, *J* = 12,4 Hz), 121.35 (s), 120.69 (s), 108.90 (s), 106.11 (d, *J* = 130.9 Hz), 32.40 (s), 26.75 (s), 21.30 (s), 20.62 (s). HRMS (EI) calcd for $C_{36}H_{42}N_3OP$: $[M]^+$ 563.306552, found 563.305600.

Analytical chiral HPLC conditions: Instrument: HP 1050; Column: Chrom Tech CHIRAL-AGP (100x4.0 mm, 5μm); eluant: acetonitrile:water 30:70, pH = 4.6-4.7 (buffer phosphate); flow rate: 0.8-1.0 mL/min ; loop: 20 μL; substrate conc.: about 1 mg/mL; detector: diode array UV detector (220 nm).

Semi-preparative HPLC resolution of 1c: Instrument: Agilent 1100 Series; column: Chrom Tech CHIRAL-AGP (150x10.0 mm, 5μm); eluant: acetonitrile:water 30:70, pH = 4.6-4.7 (buffer phosphate); flow rate: 3.8-4 mL/min; loop: 100 μL; substrate conc.: about 1 mg/mL; detector: diode array UV detector (220 nm).

About 100 injections were performed. The enantiomeric purity of all the fractions was checked by analytical HPLC under the conditions described above. The fractions displaying satisfactory enantiomeric purity (about 95%) were combined, then concentrated to dryness in vacuum, at room temperature. The solid residue was treated with dichloromethane and water. The organic layer was dried (Na_2SO_4) and evaporated to dryness under reduced pressure to give (+)-**1c** (first eluted antipode, 2.1 mg) with an enantiomeric ratio higher than 99.5% and (-)-**1**c (1.7 mg) with an enantiomeric ratio of 94.8%.

CD spectra of (+)-1c and (-)-1c: CD spectra were recorded in an about 5 10^{-4} *M* CH_2Cl_2 solution, at room temperature; cell length: 1 mm; bandwidth: 2 nm; scan speed 50 nm/min.

Dynamic ^{1}H-NMR experiments: the ^{1}H-NMR experiments carried out from room down to -90°C temperature were performed in CD_3OD solution in the case of **1a** (300 MHz), in acetone-d_6 solution in the case of **1b** (500 MHz) and in CD_2Cl_2 solution in the case of **1c** (500 MHz). The ^{1}H-NMR experiments performed from room up to 180°C temperature (**1b** and **1c**) were carried out in DMSO-d_6 (500 MHz).

Structure and Crystal Packing of Phosphine Oxides 1

1 tris(1-methyl-2-R-3-indolyl)phosphine-oxides
1a R = Me
1b R = Et
1c R = *i*-Pr

1a tris(1,2-dimethyl-3-indolyl)phosphine-oxide

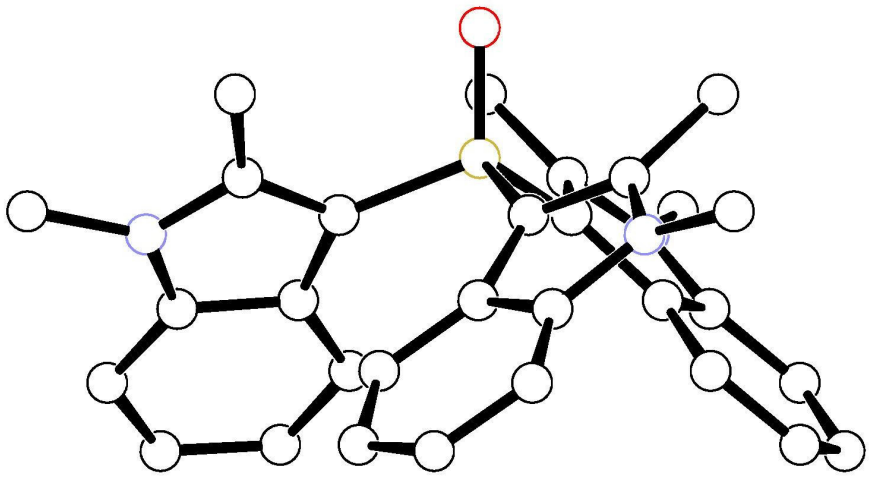

Simplified ball and stick plot of **1a** at 90 K. The molecule shows crystallographic C_3 symmetry. Hydrogen atoms omitted for clarity. Color code: black = carbon, blue = nitrogen, red = oxygen, gold = phosphorus.

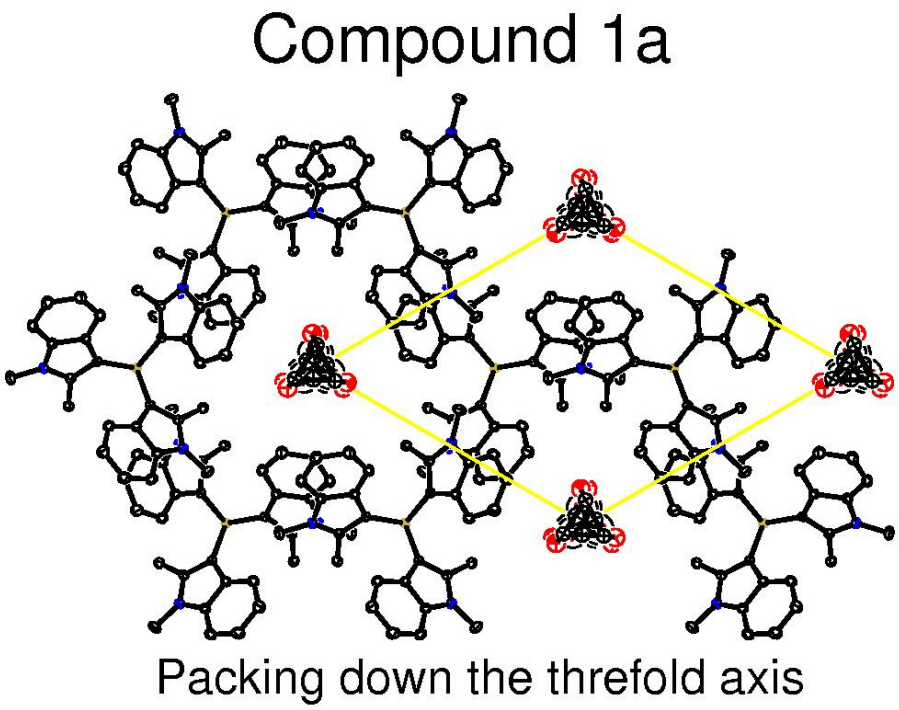

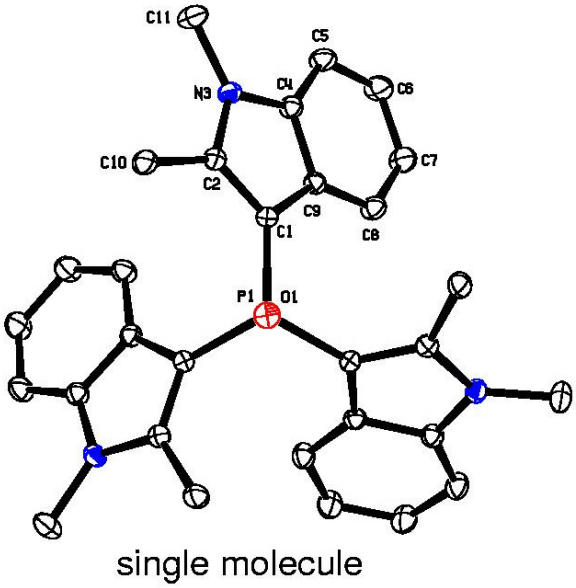

Top: packing of **1a** viewed along the *c* axis, showing the crystal channel with the disordered ethyl acetate lying along the three-fold axis at 0,0,0. Bottom: a single phosphine oxide molecule with numbering scheme. Hydrogen atoms omitted. Probability level of anisotropic displacement parameters at 50% probability level.

1b tris(2-ethyl-1-methyl-3-indolyl)phosphine-oxide

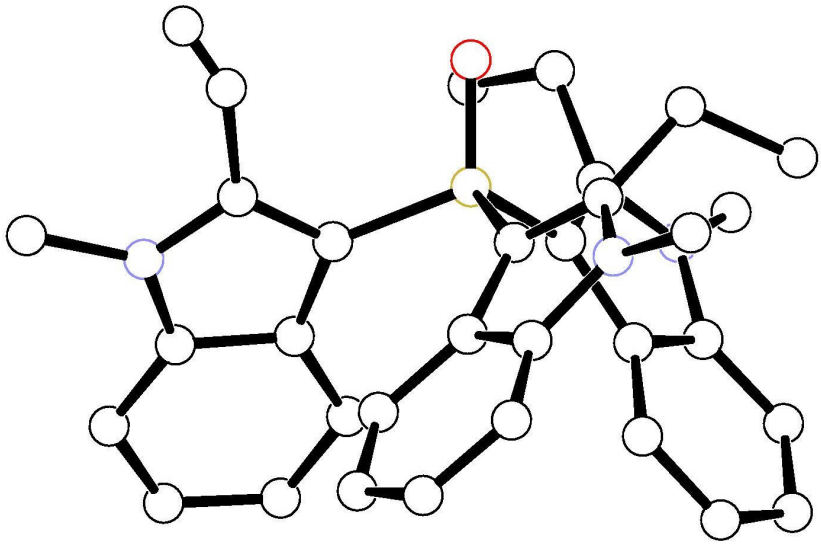

Simplified ball and stick plot of one of the two independent molecule of **1b** at 90 K. Hydrogen atoms omitted for clarity. Color code: black = carbon, blue = nitrogen, red = oxygen, gold = phosphorus. Both the independent molecules present disordered ethyl groups. The two possible conformations of such groups correspond to the positions of the isopropylic methyl groups of molecule **1c** (see below). Here only the most populated conformation is reported. It is to be noticed that **1b** and **1c** are strictly isostructural, as can be easily seen looking at their cell parameters and space group.

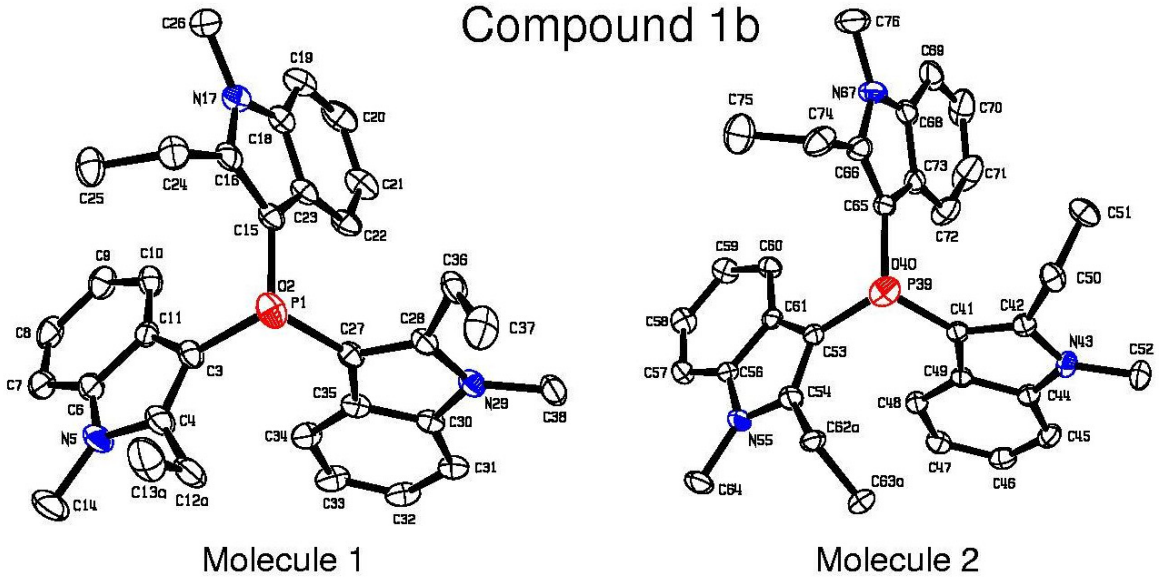

Projection along the O-P axis of the two independent molecules of **1b** with thermal parameters at 50% of probability level and numbering scheme. Only the most populated ethyl groups conformations are shown. Hydrogen atoms omitted. From the plot, it appears that the most differences are due to different torsion angles around the ethyl groups around the C(ring)-C(methylene) bonds. In fact, in molecule 2 all of the ethyl groups are nearly parallel to the plane of the three carbon atoms bonded to P, whereas in molecule 1 one is parallel and two are nearly perpendicular to the same plane. Other small differences between the two independent molecules are due to different torsion angles around the P-C bonds.

1c tris(2-isopropyl-1-methyl-3-indolyl)phosphine oxide

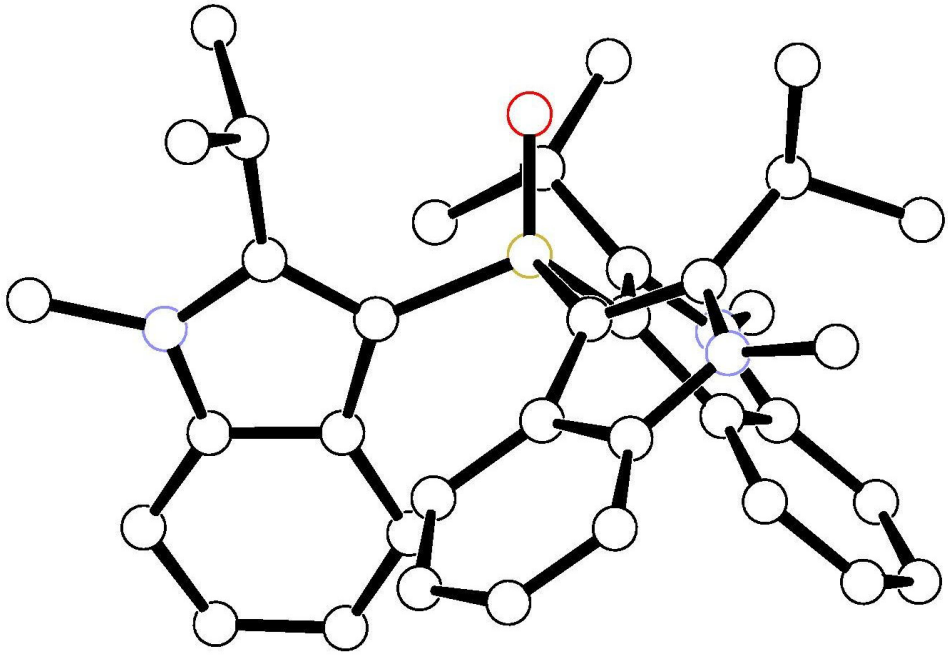

Si
mplified ball and stick plot of one of the two independent molecule of **1c** at room temperature (For this structure it was impossible to collect data at lower temperature: there probably is a phase transition that causes the crystals to break). Hydrogen atoms omitted for clarity. Color code: black = carbon, blue = nitrogen, red = oxygen, gold = phosphorus.

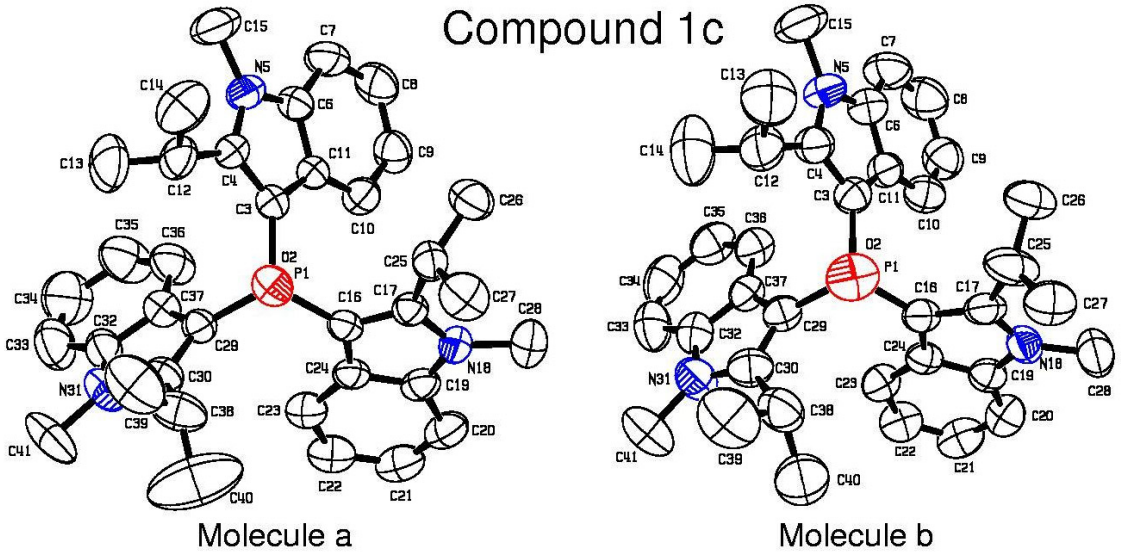

Projection along the O-P axis of the two independent molecules of **1c** with thermal parameters at 50% of probability level and numbering scheme. In molecule *b* one of the isopropyl groups (C38-C39-C40) is distributed about two preferred conformations, only one of the two is here shown. Hydrogen atoms omitted. Here the only differences between the two independent molecules are due to the torsion angles around the P-C bonds.

Density Functional Theory (DFT) Calculations

Computational Details

In order to better understand the energetics and dynamics of the present system, an extensive computational study has been carried out. We examined 12 molecular structures that fully characterize the studied phosphinoxides **1**. They are (*i*) 4 minimum energy structures, each arbitrarily chosen from the *X0*, *X1*, *X2*, and *X3* set, which suffice to characterize the whole set of minimum energy structures given the presence of enantiomer pairs and isotopomer triplets; (*ii*) 4 transition state (TS) structures for the mechanism M_0 interconverting the M*n* structures with their enantiomers P*n* (*n* = 0, 1, 2, 3); (*iii*) 4 transition state structures for the mechanism M_1 which effects the interconversion chain *P0* ⇄ *M1* ⇄ *P2* ⇄ *M3* (and its enantiomer *M0* ⇄ *P1* ⇄ *M2* ⇄ *P3*). Note that there are two non-equivalent TSs for the *M1* ⇄ *P2* process (and its enantiomer *P1* ⇄ *M2*).

This can be understood as follows. To fix the ideas, pick the *Maas* isotopomer out of the *M1* set. The M_1 mechanism comprises the operations $h.e_j$ (j = 1, 2, 3.) where h is the helicity inversion and e_j effects the orientation inversion of the j-th ring. Then $h.e_3$ converts *Maas* to *Paaa* and does not presently concern us. Instead, $h.e_2$ and $h.e_1$ correspond to the stereomerisations *Maas* → *Pass* and *Maas* → *Psas*, respectively, that have non-equivalent TSs as schematically depicted below. The M_1 operations applied to *Masa* and *Msaa* isotopomers do not spawn other non-equivalent TSs.

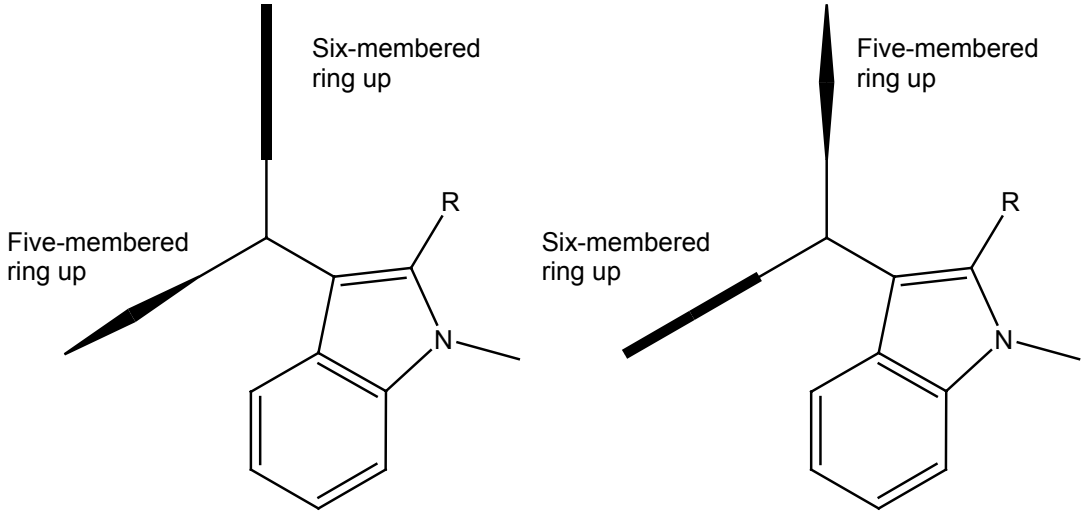

Due to the size of the studied phosphinoxide (35 heavy atoms, 278 electrons) calculations have been performed at the DFT-B3LYP/3-21G* level constraining the aromatic indole moieties to be planar; all remaining degrees of freedom have been optimized. When appropriate, C_3 symmetry has been imposed. Harmonic analysis has been carried out for all optimized structures to confirm their minimum-energy or TS nature. All calculations have been carried out by the Gaussian98 and Gaussian03 program suites.

Computational Results

The main results obtained at the DFT-B3LYP/3-21G* level are reported in the following Tables.

Tris(1,2-dimethyl-3-indolyl)phosphine oxide **1a**

Isomer	*X3*	*X2*	*X1*	*X0*
E / au	-1732.818804	-1732.813774	-1732.808613	-1732.804130
ΔE / kcalmol	**0.0**	**3.2**	**6.4**	**9.2**
P	**98.6%**	**1.4%**	**0.0%**	**0.0%**

TS of M_0 = h	**E / au**	**ΔE/kcalmol**	**ΔG/kcalmol**
X3 → X'3	-1732.781365	**23.5**	**25.0**
X2 → X'2	-1732.780422	**20.9**	**23.9**
X1 → X'1	-1732.776644	***20.1***	***22.2***
X0 → X'0	-1732.768829	**22.2**	**23.8**

TS of M_1 = h.e_i	**E / au**	**ΔE/kcalmol**	**ΔG/kcalmol**
X3 → X'2	-1732.806246	**7.9**	**9.1**
X2 → X'1	-1732.802335	**7.2**	**8.4**
X2 → X'1	-1732.805597	**5.1**	**7.0**
X1 → X'0	-1732.799058	**6.0**	**8.5**
X2 → X'3	-1732.806246	**4.7**	**6.9**
X1 → X'2	-1732.802335	**3.9**	**5.2**
X1 → X'2	-1732.805597	**1.9**	**3.8**
X0 → X'1	-1732.799058	**3.2**	**7.2**

N.B.: $X, X' = M, P$, with $X \neq X'$.

The most significant structures of **1a** are pictured below

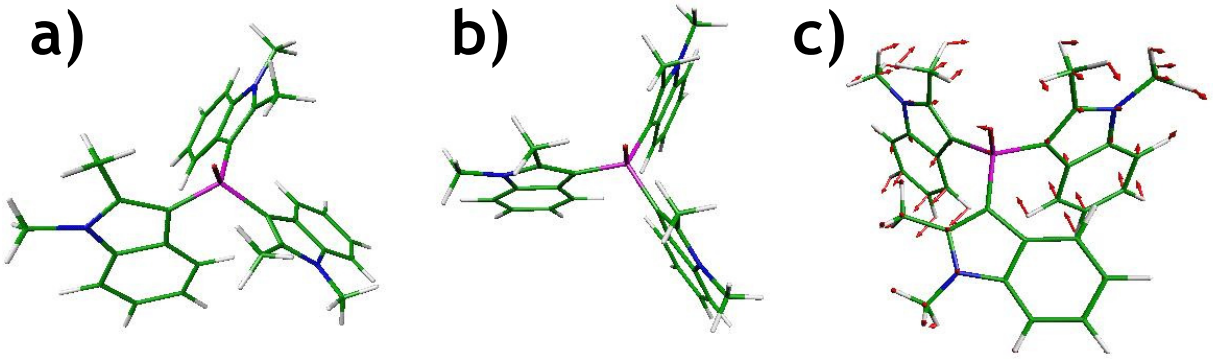

B3

LYP/3-21G* optimized structures of selected stereoisomers of tris(1,2-dimethyl-3-indolyl)phosphine oxide **1a**. a) *M3* isomer; b) transition state of the M_0 isomerisation from *M3* to *P3*; c) transition state of the M_1 isomerisation from *M3* to *P2*. In the latter subpanel red arrows show the isomerisation eigenvector, *i.e.*, that with negative eigenvalue.

For **1b** and **1c**, only the transition states involving the major *X3* isomers have been computed

Tris(2-ethyl-1-methyl-3-indolyl)phosphine oxide **1b**

Isomer	*X3*	*X2*	*X1*	*X0*
E / au	-1850.12306	-1850.117235	-1850.108033	-1850.10114
DE / kcalmol	**0.0**	**3.7**	**9.4**	**13.8**
P	**99.4%**	**0.6%**	**0.0%**	**0.0%**

TS of M_0 = h	**E / au**	**ΔE/kcalmol**	**ΔG/kcalmol**
X3 → *X'3*	-1850.083629	**24.7**	**26.6**

TS of M_1 = h.e$_i$	**E / au**	**ΔE/kcalmol**	**ΔG/kcalmol**
X3 → *X'2*	-1850.108521	**9.1**	**12.1**
X2 → *X'3*	-1850.108521	**5.5**	**3.1**

Tris(2-isopropyl-1-methyl-3-indolyl)phosphine oxide **1c**

Isomer	*X3*	*X2*	*X1*	*X0*
E / au	-1967.41753	-1967.412905	-1967.407179	-1967.40332
DE / kcalmol	**0.0**	**2.9**	**6.5**	**8.9**
P	**97.8%**	**2.2%**	**0.0%**	**0.0%**

TS of M_0 = h	**E / au**	**ΔE/kcalmol**	**ΔG/kcalmol**
X3 → *X'3*	-1967.371155	**29.1**	**34.5**

TS of M_1 = h.e$_i$	**E / au**	**ΔE/kcalmol**	**ΔG/kcalmol**
X3 → *X'2*	-1967.403816	**8.6**	**9.7**
X2 → *X'3*	-1967.403816	**5.7**	**8.8**

Fitting of Chiral HPLC Chromatograms

Theory & Methods

In chiral HPLC experiments carried out on tris(1,2-dimethyl-3-indolyl)phosphine oxide **1a**, dynamical effects are observed that are attributed to the enantiomerization of the residual enantiomers, i. e., to the dynamical equilibrium brought about by M_0 isomerisation. As a theoretical framework to interpret these experiments, we used the stochastic model [R. A. Keller and J. C. Giddings, *J. Chromatog.*, **3** (1960) 205-220] that is amenable to a rigorous analytical treatment. Although this theory has been reported several times in the literature, [R. Kramer, *J. Chromatog.*, **107** (1975) 241-252; J. Veciana and M. I. Crespo, *Angew. Chem. Int. Ed. Engl.*, **30** (1991) 74-76; O. Trapp, G. Schoetz and V. Schurig, *Chirality*, **13** (2001) 403-414; O. Trapp and V. Schurig, *Comput. Chem.*, **25** (2001) 187-195] we think that a concise outline might be a useful reference for the reader.

For the sake of clarity, we begin considering a simple chemical exchange between species A and B that occurs in the mobile phase with rate constants k_{AB} and k_{BA}, and is much slower than the solute exchange between mobile and stationary phases. The chromatographic profile is best described as

$$P(t) = P_A(t) + P_B(t) + P_{AB}(t), \tag{1}$$

where P_A and P_B are due to molecules that did not undergo exchange during elution and P_{AB} is due to molecules that underwent one or more exchanges during elution. In the linear, ideal case, one can write

$$P_A(t) = \begin{cases} c_A \exp(-k_A t), & \text{for } t = t_A \\ 0, & \text{otherwise} \end{cases} \tag{2}$$

and similarly for B, where t_A is the retention time and c_A is the initial amount of species A, and the chromatographic peak is infinitely narrow. For the exchange part one can write

$$P_{AB}(t) = \begin{cases} \left[(c_A k_A + c_B k_B)\, I_0(2\hat{k}t) + \sqrt{k_A k_B}\,(c_A r + c_B / r)\, I_1(2\hat{k}t) \right] t \exp(-\bar{k}t), & \text{for } t_A < t < t_B \\ 0, & \text{otherwise} \end{cases}, \tag{3}$$

where I_0 and I_1 are modified Bessel functions of the first kind, $r = [x/(1-x)]^{1/2}$, and

$$x = \frac{t_B - t}{t_B - t_A} \frac{t_A}{t} \tag{4}$$

is the fraction of time that a molecule eluting at time t spends as species A. Note that the effective retention time t for a molecule which underwent one or more enantiomerizations is *not* linearly related to the time fraction x. The averaged rate constants are

$$\bar{k} = xk_{\mathrm{A}} + (1-x)k_{\mathrm{B}}, \quad \hat{k} = \sqrt{xk_{\mathrm{A}}(1-x)k_{\mathrm{B}}}\,. \tag{5}$$

The particular dynamic process we are dealing with, i.e. enantiomerisation of a racemic mixture, is in some respect a special case of chemical exchange (e. g., $c_{\mathrm{A}} = c_{\mathrm{B}}$) but it also bears some differences. Indeed, if an enantiomeric resolution is performed by chiral stationary phase chromatography, then we have to distinguish between enantiomerisation rate constants in the mobile and stationary phase:

$$k_{\mathrm{A}}^{\mathrm{m}} = k_{\mathrm{B}}^{\mathrm{m}} \equiv k^{m} \neq k_{\mathrm{A}}^{\mathrm{s}} \neq k_{\mathrm{B}}^{\mathrm{s}}. \tag{6}$$

The above equations are still valid provided that k_{A} and k_{B} denote apparent rate constants defined as

$$k_{\mathrm{A}} = \frac{k^{m} + k'_{\mathrm{A}} k_{\mathrm{A}}^{\mathrm{s}}}{1 + k'_{\mathrm{A}}}, \tag{7}$$

and similarly for B, where k'_{A} is the retention factor of A. Knowledge of k_{A}, k_{B}, t_{A}, t_{B}, and the mobile phase hold-up time t_{M}, which can be obtained from the experimental data, allows one to compute the mechanistic rate constants k^{m}, $k_{\mathrm{A}}^{\mathrm{s}}$, and $k_{\mathrm{B}}^{\mathrm{s}}$.

The linear ideal profiles are made realistic by convolution with an appropriate peak shape model. After an extensive survey, we found that the most capable and flexible peak shape function is the exponentially-transformed Gaussian (ETG) function. [J. Li, *Anal. Chem.*, **69** (1997) 4452-4462] The peak shape parameters **p** (width, asymmetry, etc.) used to convolve P_{A} and P_{B} are those of the pure residual enantiomers $\mathbf{p}_{\mathrm{A}}$ and $\mathbf{p}_{\mathrm{B}}$. Which peak shape parameters should be employed for the time-extended exchange profile P_{AB}? Conventional use of mean values $\mathbf{p} = (\mathbf{p}_{\mathrm{A}}+\mathbf{p}_{\mathrm{B}})/2$ for the whole P_{AB} profile leads to artifacts, since a variation of the peak parameters across the P_{AB} profile is expected. In their SM+ model, Trapp and Schurig [O. Trapp and V. Schurig, *Comput. Chem.*, **25** (2001) 187-195] proposed the linear variation $\mathbf{p} = \mathbf{p}_{\mathrm{A}} + (\mathbf{p}_{\mathrm{B}}-\mathbf{p}_{\mathrm{A}})(t-t_{\mathrm{A}})/(t_{\mathrm{B}}-t_{\mathrm{A}})$ of the peak parameters with the P_{AB} profile. Although this surely is an improvement, we find it more physically sound using a linear variation of the parameters with respect to the time fraction spent as A. Hence, we used $\mathbf{p} = x\mathbf{p}_{\mathrm{A}} + (1-x)\mathbf{p}_{\mathrm{B}}$.

The above outlined chromatogram model has been implemented in a Matlab script. The chromatograms recorded at temperatures between 0° and 70° have been fitted one at a time, obtaining, among other, the best-fit values of k^{m}, $k_{\mathrm{A}}^{\mathrm{s}}$, and $k_{\mathrm{B}}^{\mathrm{s}}$ as a function of temperature. Their errors have been estimated at the 90% confidence level by a bootstrap procedure with 101 samples. Rate constants have then been fitted to the Eyring equation

$$k = \frac{k_{Boltz}T}{h}\exp\left(-\Delta G^{\ddagger}/k_{Boltz}T\right) = \frac{k_{Boltz}T}{h}\exp\left(-\Delta H^{\ddagger}/k_{Boltz}T\right)\exp\left(\Delta S^{\ddagger}/k_{Boltz}\right) \tag{8}$$

to get the activation enthalpy and entropy.

CD-detected HPLC experiments do not show dynamical effects since the opposite sign of the CD for the residual enantiomers almost deletes the P_{AB} profile. The P_A and P_B profiles (with opposite sign) have been subjected to a similar fitting procedure, obviously without the dynamical part. Because of the less demanding nature of fitting CD-detected chromatograms, a simpler peak shape function has been used, namely, the Gaussian-joined-exponential function (GJE) that we here introduce:

$$\mathrm{GJE}(t) = \begin{cases} N_1 \exp\left[-(t-t_R)^2/2\sigma^2\right], & N_1 = \dfrac{C}{CA_1 + A_2}, \\ N_2 \exp(-t/\tau), & N_2 = \dfrac{1}{CA_1 + A_2}, \end{cases} \qquad \begin{aligned} C &= \exp\left(-t_R/\tau - \sigma^2/2\tau^2\right) \\ A_1 &= \sigma\sqrt{\frac{\pi}{2}}\left[1 + \mathrm{erf}\left(\frac{t-t_0}{\sigma\sqrt{2}}\right)\right] \\ A_2 &= \tau\exp\left(-t_0/\tau\right) \end{aligned} \tag{9}$$

It is a normalized function obtained by joining a leading Gaussian and a trailing exponential at the unique time point t_0 where the first derivatives are equal ($t_0 = t_R + \sigma^2/\tau$, where t_R is the retention time, σ is the standard deviation of the Gaussian, and τ is the exponential decay time).

Circular-Dichroism Detected Chiral HPLC

Dynamical effects are largely quenched in CD-detected chromatograms because of the opposite sign of the CD for the residual enantiomers. The room temperature chromatograms of tris(1,2-dimethyl-3-indolyl)phosphine oxide **1a** detected at 230 and 280 nm are reported in the Figure along with the best-fit profiles. The opposite sign of the CD of the two peaks is clear evidence that the they represent an enantiomer pair. The calculated profiles fit well the experimental ones except for the interval between the peaks where the cancellation of the opposite CD signals is not complete. The best-fit parameters are reported in the Table below along with their errors at the 90% confidence level. The retention times and the width of the trailing peak are reproducible between the two experiments.

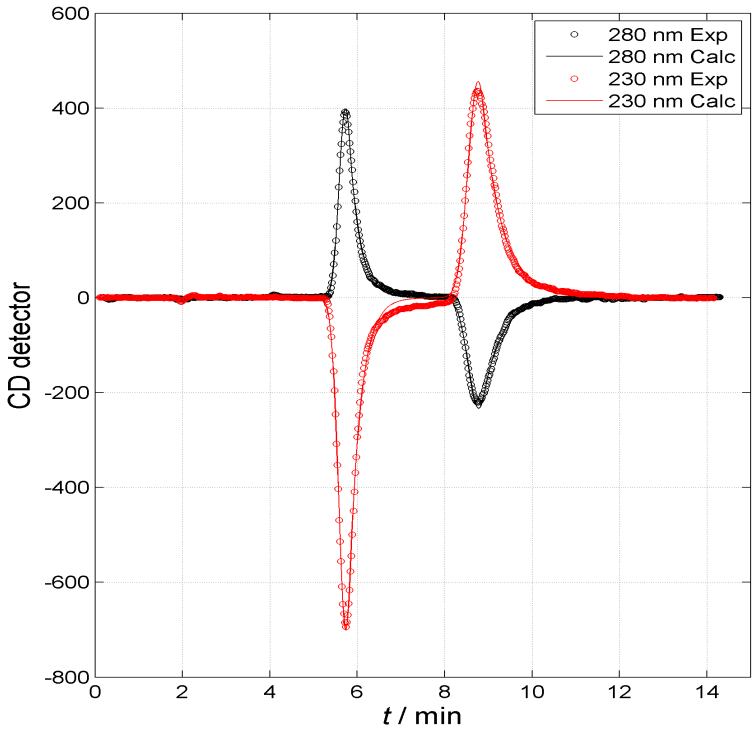

Table. Best-fit retention times t_R and widths of leading gaussian edge (σ) and of the trailing exponential edge (τ) in minutes from the CD-detected chromatograms of tris(1,2-dimethyl-3-indolyl)phosphine oxide **1a**.

		1st eluted	**2nd eluted**
CD @ 280 nm	t_R / min	5.730 ± 0.006	8.775 ± 0.006
	σ / min	0.145 ± 0.004	0.239 ± 0.009
	τ / min	0.242 ± 0.007	0.43 ± 0.02
CD @ 230 nm		**1st eluted**	**2nd eluted**
	t_R / min	5.737 ± 0.003	8.76 ± 0.01
	σ / min	0.165 ± 0.002	0.227 ± 0.008
	τ / min	0.255 ± 0.008	0.45 ± 0.01

Variable-temperature Ultraviolet-Detected Chiral HPLC

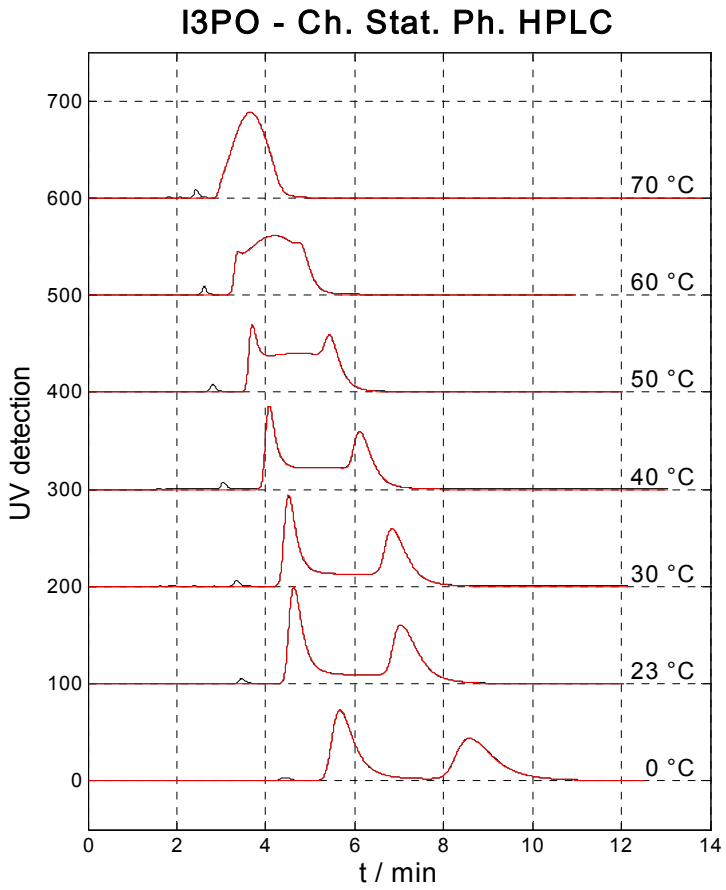

The UV-detected, variable-temperature chromatograms of tris(1,2-dimethyl-3-indolyl)phosphine oxide **1a** are reported in the Figure (black line) along with the best-fit profiles (red line). They cover the whole dynamical range from the almost static regime at 0 °C to the fast-exchange regime at 70 °C where the peaks have coalesced. At intermediate temperatures the plateau typical of interconversion dynamics is clearly seen growing in intensity on rising temperature. Both static and dynamical chromatographic parameters have been extracted from the experimental data by a fitting procedure based on the stochastic model specialized for an enantiomerisation process. These are reported in the Table along with their errors at the 90% confidence limit.

Table. Best-fit retention times t_R and rate constants for the enantiomerisation processes in the mobile (k_m) and chiral stationary phase (k_{12s} and k_{21s}) of tris(1,2-dimethyl-3-indolyl)phosphine oxide **1a** obtained from the variable-temperature UV-detected chromatograms (eluent water:ACN 3:1).

T / °C	$t_{R,1}$ / min	$t_{R,2}$ / min	1000 k_m / s^{-1}	1000 k_{12s} / s^{-1}	1000 k_{21s} / s^{-1}
0	5.86 ± 0.04	7.61 ± 0.07	–	–	–
23	4.73 ± 0.02	6.87 ± 0.08	0.006 ± 0.001	0.007 ± 0.002	0.004 ± 0.001
30	4.58 ± 0.02	6.7 ± 0.1	0.010 ± 0.003	0.012 ± 0.004	0.007 ± 0.002
40	4.13 ± 0.03	5.9 ± 0.1	0.03 ± 0.01	0.030 ± 0.009	0.018 ± 0.006
50	3.78 ± 0.04	5.2 ± 0.1	0.09 ± 0.04	0.09 ± 0.03	0.05 ± 0.02
60	3.50 ± 0.08	4.3 ± 0.1	0.19 ± 0.06	0.22 ± 0.06	0.15 ± 0.05
70	3.2 ± 0.1	3.8 ± 0.2	0.6 ± 0.2	0.5 ± 0.1	0.4 ± 0.1

In the chiral stationary phase the 1 → 2 enatiomerization is always faster than the reverse 2 → 1 step, in agreement with the fact that residual enantiomer 2 elutes later than 1. The enatiomerization rate constant in the mobile phase has intermediate velocity, except at high temperature. The temperature dependence of the rate constants has been fit to the Eyring equation (8). The results are shown in the following Table and exemplified in the Figure below.

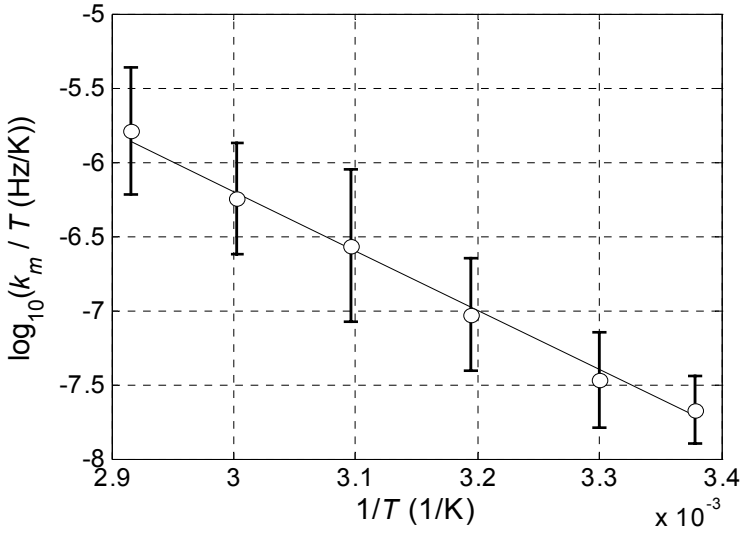

Table. Best-fit Eyring activation enthalpy ($\Delta H^{\ddagger}$) and entropy ($\Delta S^{\ddagger}$) for the enantiomerisation processes of tris(1,2-dimethyl-3-indolyl)phosphine oxide **1a**. The goodness of fit measures are the correlation coefficient and the χ^2 significance.

Process	$\Delta H^{\ddagger}$ / kcal mol^{-1}	$\Delta S^{\ddagger}$ / cal mol^{-1} K^{-1}	Corr. Coeff.	$Q(\chi^2)$
Mobile phase	18.3 ± 0.7	-21 ± 2	-0.997	0.71
1 → 2, stationary phase	17.9 ± 0.7	-22 ± 2	-0.999	0.64
2 → 1, stationary phase	18.8 ± 0.8	-20 ± 2	-0.997	0.93

Whereas the differences between the various processes are not statistically significant, the enantiomerisation process as a whole is well characterized thanks to the high quality of the fit. It has an activation enthalpy of 18–19 kcal/mol which witnesses the strong overcrowding present in this phosphinoxide; the negative activation entropy indicates loss of motional freedom in the transition states.

Fitting of Dynamical ^{1}H-NMR Line Shape

The theory of dynamic NMR spectroscopy has been summarized many times.[G. Binsch in *Dynamic Nuclear Magnetic Resonance Spectroscopy*, Eds. L. M. Jackman and F. A. Cotton, Academic Press, New York, 1975; R. R. Ernst, G. Bodenhausen and A. Wokaun, *Principles of Nuclear Magnetic Resonance in One and Two Dimensions*, Clarendon Press, Oxford, 1991; M. H. Levitt, *Spin Dynamics*, J. Wiley and Sons, New York, 2001] The transverse components of the magnetization of spin systems that can be treated to first-order and that undergo (possibly pseudo) first-order exchange reactions follow the equation of motion

$$\frac{d}{dt}\vec{M}^{+} = \mathbf{L}\,\vec{M}^{+} \tag{10}$$

where transitions in all M exchanging sites and the Liouvillian matrix is

$$\mathbf{L} = i\,\mathbf{\Omega} - \mathbf{\Lambda} + \mathbf{K} \tag{11}$$

where the elements of the diagonal matrix $\mathbf{\Omega}$ correspond to the frequency $\Omega_{pm,pm}$ of the p-th transition in the m-th site and $\mathbf{\Lambda}$ is the transverse relaxation matrix with elements $\Lambda_{pm,qn}$. $\mathbf{\Lambda}$ is usually assumed diagonal with elements

$$\Lambda_{pm,qn} = \delta_{pq}\,\delta_{mn}\;T_{2,p}^{-1}, \tag{12}$$

but off-diagonal elements between degenerate transitions may occur. $\mathbf{K}$ is the kinetic matrix with elements

$$K_{pm,qn} = \delta_{pq}\,k_{nm}, \quad m \neq n \quad \text{and} \quad K_{pm,pm} = -\sum_{m\neq n} k_{mn} \tag{13}$$

where k_{mn} is the rate constant for the reaction from site m to site n. At equilibrium, the equation of motion simplifies to

$$\mathbf{L}\vec{M}^{+} \equiv \left(i\,\mathbf{\Omega} - \mathbf{\Lambda} + \mathbf{K}\right)\vec{M}^{+} = 0 \tag{14}$$

so that the transverse magnetization vector is obtained by diagonalizing the complex symmetric matrix $\mathbf{L}$. The complex eigenvalues of $\mathbf{L}$ give the frequency and width of the transitions, while the eigenvectors determine their intensity and phase.

The usual procedure is as follows; i) each spectrum is fitted within the framework of the above outlined theory, thus obtaining the desired rate constant at each temperature; ii) the activation barrier parameters, i.e., $\Delta H^{\ddagger}$ and $\Delta S^{\ddagger}$, are obtained from fitting the rate constants to the Eyring equation (Eq. 8). Here we used a numerically more balanced and better performing procedure consisting in fitting all

spectra at once to a theoretical model obtained by merging the dynamical NMR theory with Eyring equation. Among the optimized fit parameters, one finds the activation parameters $\Delta H^{\ddagger}$ and $\Delta S^{\ddagger}$. This global procedure has been implemented in a Matlab script exploiting the Nelder-Mead Simplex method, a rather slow but very robust algorithm that relies only on the value of the target function (the sum of the squared difference between the experimental and the calculated line-shape) and does not need evaluation of the derivatives of the target function with respect to the fit parameters. The errors affecting the optimized parameters (at the 68.3% confidence level) have been evaluated by a bootstrap procedure.